



MOX–Report No. 54/2014

**Uncertainties in renewable energy generation systems:
functional data analysis, monte carlo simulation, and
fuzzy interval analysis**

FERRARIO, E.; PINI, A.

MOX, Dipartimento di Matematica “F. Brioschi”
Politecnico di Milano, Via Bonardi 9 - 20133 Milano (Italy)

mox@mate.polimi.it

<http://mox.polimi.it>

Uncertainties in Renewable Energy Generation Systems: Functional Data Analysis, Monte Carlo Simulation, and Fuzzy Interval Analysis

E. Ferrario^a, A. Pini^b

^a Chair on Systems Science and the Energetic Challenge,
European Foundation for New Energy - Electricité de France,
École Centrale Paris - Supelec, France

`elisa.ferrario@ecp.fr`

^b MOX– Modellistica e Calcolo Scientifico
Dipartimento di Matematica “F. Brioschi”
Politecnico di Milano

`alessia.pini@mail.polimi.it`

Keywords: Photovoltaic Energy, Irradiation, Functional Data Analysis, Fuzzy Interval Analysis, Monte Carlo Simulation.

AMS Subject Classification: 03E72, 62M15, 62M10, 62P12.

Abstract

In this paper, aleatory and epistemic uncertainties in energy generation systems are investigated. The former are described by probability distributions, whereas the latter by possibility distributions. In particular, time-varying probability distributions elicited by Functional Data Analysis are considered for the representation of the aleatory uncertainty that evolves with time. Then, the joint propagation of both types of uncertainty is performed by Monte Carlo simulation and Fuzzy Interval Analysis. The method is applied to a model of an energy system made of a solar panel, a storage energy system and the loads. As a quantitative indicator of the analysis we evaluate the Expected Energy Not Supplied.

1 Introduction

Renewable energy is getting more and more important as a solution for the climate change concerns. However, it is affected by large uncertainties, due to the intermittent nature of the energy source (actually, regardless of the type of

renewable source, the amount of energy daily available can present high variations from one day to another, at the same site) Borges (2012). In addition, a long-term prediction of the energy that is daily available is a difficult problem, due to the complexity of the system at hand. These issues mine the reliability of the renewable energy, making it difficult to completely rely on it.

In this respect, we propose a methodology that deals with uncertainties in renewable energy generation. In particular, we consider two types of uncertainty: randomness due to inherent variability in the system behavior (aleatory uncertainty) and imprecision due to lack of knowledge and information on the system (epistemic uncertainty) as typically distinguished in system risk analysis Helton and Oberkampf (2004). As illustrated in recent works of risk analysis Li and Zio (2012), we address the co-existence of aleatory and epistemic uncertainties in the reliability assessment of a distributed generation system by representing the aleatory variables as probabilistic and the epistemic ones as possibilistic.

Traditionally, aleatory uncertainty of an energy distribution system is represented by a unique probability density function that is inferred from historical data of one fixed period Li and Zio (2012); Baraldi and Zio (2008). Nevertheless, the data distribution evolve through time in a continuous way. Here we propose to consider that time variation within a Functional Data Analysis (FDA) framework Ramsay and Silverman (2002, 2005); Ferraty and Vieu (2006), where data are represented as functions of a continuous variable, which is time in our application. By applying FDA methods, it is then possible to model the entire time evolution of data. We propose to analyze this time evolution in order to obtain more realistic results from the uncertainty analysis. If we neglect long-term climatic changes, we may assume that this time evolution is one-year periodic. Hence, in this work, we model climatic data as random samples from parametric distributions with one-year periodic parameters. Finally, we propagate the aleatory and epistemic uncertainty by means of a hybrid approach that combines Monte Carlo Simulation and Fuzzy Interval Analysis Li and Zio (2012); Baraldi and Zio (2008).

To exemplify the methodology, we analyze the aleatory and epistemic uncertainties of a model of a photovoltaic energy distribution system made of a solar panel, a storage energy system (that stores the generated energy exceeding the demand of the end-users) and loads (power demanded by the end-users). As a quantitative indicator of the analysis we evaluate the Expected Energy Not Supplied, a reliability index commonly used in this field Billinton et al. (1984). The results of the uncertainty propagation in the case study are compared with: *i*) the pure probabilistic uncertainty propagation approach based on the same time-varying distributions Marseguerra and Zio (2002); and *ii*) the Monte Carlo Simulation and Fuzzy Interval Analysis approach considering the random variables constant in time, i.e. described by a unique probability density function.

The remainder of the paper is organized as follows. In Section 2, the Functional Data Analysis methods adopted for the modeling of time-varying data and the Monte Carlo and Fuzzy Interval Analysis approach used for the joint

uncertainty propagation are detailed. In Section 3 the case study that we will analyze is presented. In Section 4, the results are reported and commented; finally, in Section 4, conclusions are provided. Some details on the joint uncertainty propagation, and on the time-varying estimate of the load are reported in Appendices A and B, respectively.

2 Methodology

The methodology that we propose to evaluate uncertainties in renewable energy generation is based on the joint modeling and propagation of all the uncertainties of the model, that can be either aleatory or epistemic. The first step in order to evaluate the uncertainties in renewable energy generation consists in modeling the system of energy generation, listing all sources of uncertainty in the model inputs (e.g., electricity demand) that propagate to the model output (e.g. electricity supply). These sources of uncertainty can be distinguished into two types: epistemic uncertainties (due to lack of knowledge, and for which no historical data are available) and aleatory uncertainties (due to the intrinsic variability of the system, typically modeled by means of large amounts of historical data). The former type of uncertainty is also referred to as “reducible” uncertainty to highlight that a gain of information about the system can lead to a reduction of epistemic uncertainty. In renewable energy applications, epistemic uncertainty typically characterizes the parameters of the devices due to i) the lack of information provided by the manufacturers for commercial reasons and ii) the limited quantity of data available for each house for private issues Izquierdo et al. (2011).

Aleatory uncertainties can instead be due to the variability of the energy source (e.g., wind speed and direction, solar irradiation) and the loads (i.e., power demanded by the end-users). In the current risk assessment practice, both types of uncertainties are represented by means of probability distributions with fixed parameters. However, potential limitations are associated to a probabilistic representation of epistemic uncertainty under limited information Helton and Oberkampf (2004) and a number of alternative representation frameworks have been proposed, e.g., fuzzy set theory, evidence theory, possibility theory and interval analysis Klir and Yuan (1995); Aven and Zio (2011). Given the representation power of possibility theory and its relative mathematical simplicity, we adopt it to describe the epistemic uncertainty in renewable energy applications. In addition, we represent the aleatory uncertainty by means of time-varying probability distributions since the variables associated with renewable energy systems can vary with time (e.g., day and night, seasons, etc.). For instance, the solar irradiation in summer is higher than in winter; as a consequence, the mean of its probability distribution should change with seasons (i.e., it should be higher in summer and lower in winter). The parameters of these time-varying probability distributions have been evaluated from historical

data by applying FDA techniques.

Finally, the aleatory and epistemic uncertainties are jointly propagated on the renewable energy system by combining Monte Carlo simulation and Fuzzy Interval Analysis. Actually, the possibilistic representation of uncertainty can both be combined with and transformed into the traditional probabilistic representation. In the following subsections we present the details of the methodology adopted to model the time-varying data distribution, and propagate the aleatory and epistemic uncertainties from the input variables of the system to the output variable of interest.

2.1 Uncertainty modeling of time-varying data

Suppose to observe n realizations of the quantity of interest ξ (e.g., irradiation, wind speed) for the chosen location through time, during the year: for each time unit t_q (i.e., a day), we observe n different samples of functional data $\xi_i(t_q)$, where $i = 1, \dots, n$ denotes the sample units, and $q = 1, \dots, Q$ denotes the different time units. We suppose that, for a fixed time t_q , the observed data $\xi_i(t_q)$ is a random independent sample from a fixed parametric distribution $F_{\boldsymbol{\eta}}$, described by a set of unknown parameters $\boldsymbol{\eta}(t_q) \in \mathbb{R}^r$:

$$\xi_i(t_q) \sim F_{\boldsymbol{\eta}}, \quad \forall i = 1, \dots, n, q = 1, \dots, Q. \quad (1)$$

The distribution $F_{\boldsymbol{\eta}}$ can be chosen in different ways, according to the data that we are modeling. For instance, a Beta distribution is typically used to model solar irradiation, while a Weibull distribution is used to model wind speed Atwa et al. (2010); Li and Zio (2012); Salameh et al. (1995).

We assume that observations on different time units are conditionally independent, given the values of the parameters $\boldsymbol{\eta}$. In particular, this implies that the dependence structure of the solar irradiation on different days is entirely expressed by means of the time-varying structure of its parameters, which we suppose can be modeled as smooth and regular functions of time, due to the intrinsic regularity of data.

To estimate the time-varying parameters we adopt, for each time unit t_q , the method of moments. So, to elicit a time-varying estimate for the distribution of data, we only need to find time-varying estimates for the first r moments of the distribution of data. Furthermore, we suppose that the moments of the distribution are regular one year-periodic functions. Since the sample daily moments are extremely non-regular functions, we consider a method to regularize data, estimating a proper low dimensional functional space in which they are defined, by exploiting the procedure proposed in Pini and Vantini (2013). In the following, we describe the smoothing procedure applied to estimate the r th moment of data distribution.

2.1.1 Estimate of time-varying moments

Suppose that we want to estimate the moment of order r of the data distribution, $r \geq 1$. Let $\varphi_i(t) = \xi_i(t)^r$. We need to estimate the mean of functions $\varphi_i(t)$. We apply a Fourier-based Interval Testing Procedure (ITP) described in Pini and Vantini (2013). The method consists in the following three steps:

1. **Basis Expansion:** functional data (in our case: time-varying irradiation data) are represented through the coefficients of a truncated ordered basis expansion;
2. **Interval-Wise Testing:** a suitable test is performed on each interval of ordered basis coefficients;
3. **Multiple Correction:** for each component of the basis expansion, an adjusted p -value is computed from the p -values of the tests performed in the previous step.

The final result of the procedure is a family of adjusted p -values, one for each basis function used in the expansion. This result can be used to select the basis components that are statistically significant to describe the mean function of data (for instance, selecting all the components with associated adjusted p -value lower than the 5% level).

In our application, data are assumed to be one-year periodic functions. Hence, a natural choice for the basis used to describe data is the one-year periodic Fourier basis. In detail, we use an interpolating Fourier expansion:

$$\varphi_i(t_q) = \frac{a_i^{(0)}}{2} + \sum_{h=1}^{(Q-1)/2} a_i^{(h)} \cos\left(\frac{2\pi}{Q}ht_q\right) + b_i^{(h)} \sin\left(\frac{2\pi}{Q}ht_q\right), \quad Q = 365. \quad (2)$$

In the case of a Fourier basis expansion, intervals of basis components are frequency bands. In detail, equation (2) associates at each data, and for each frequency $h > 0$, a bivariate vector of coefficients $(a_i^{(h)}, b_i^{(h)})$, and for the frequency $h = 0$ a coefficient $a_0^{(h)}$. Denote as $(A^{(h)}, B^{(h)})'$ the bivariate distribution of coefficients $(a_i^{(h)}, b_i^{(h)})$ (and $A^{(0)}$ the distribution of the 0th frequency). For each frequency $h > 0$, the ITP can be applied to associate an adjusted p -value to each of the following bivariate tests:

$$H_0^{(h)} : \mathbb{E} \left[(A^{(h)}, B^{(h)})' \right] = (0, 0)' \text{ vs. } H_1^{(h)} : \mathbb{E} \left[(A^{(h)}, B^{(h)})' \right] \neq (0, 0)', \quad (3)$$

while for the 0th frequency, an adjusted p -value to the univariate test:

$$H_0^{(0)} : \mathbb{E} [A^{(0)}] = 0 \text{ vs. } H_1^{(0)} : \mathbb{E} [A^{(0)}] \neq 0, \quad (4)$$

In particular, by means of tests (3)-(4), we aim at selecting the frequencies that are significantly different from zero in the expansion of the mean signal. The

final time-varying estimate of the mean function will then be evaluated as the Fourier basis expansion on these frequencies.

In order to apply the ITP, we then need to specify how to perform the interval-wise tests of the second phase of the procedure, that is in our case, how to perform a test on each frequency band. In detail, we need a test for each frequency (single-frequency tests), and a test for each interval of frequencies (multiple-frequency test). The approach that we use to perform such tests is a non-parametric approach based on the suitable combination of joint permutation tests on each frequency. We start by performing each single-frequency test, by means of permutation tests Pesarin and Salmaso (2010). For each frequency $h > 0$ we perform a bivariate test to test the null hypothesis $\mathbb{E}[(A^{(h)}, B^{(h)})] = (0, 0)$, based on the joint changes of the signs of vectors $(a_i^{(h)}, b_i^{(h)})$ and on the Hotelling T^2 statistic $T(\mathbf{a}^{(h)*}, \mathbf{b}^{(h)*}) = (\bar{a}^{(h)*}, \bar{b}^{(h)*})' S_{h,h}^* (\bar{a}^{(h)*}, \bar{b}^{(h)*})$, where $(\mathbf{a}^{(h)*}, \mathbf{b}^{(h)*})$ denote the permuted data, and $S_{h,h}^* \in \mathbb{R}^{(2 \times 2)}$ is the covariance matrix of permuted data at frequency h . For the 0th frequency, we perform a univariate permutation test based on the squared of the univariate Student t statistic and on the change of the signs of the coefficients $a_i^{(0)}$. It is important to note here that the permutations used to build the single-frequency tests are the same across frequency. This aspect will be key to build the multiple-frequency tests.

To perform multiple-frequency tests, we combine the results of the single-frequency tests by means of the non-parametric combination (NPC) methodology, based on the Fisher combining function Pesarin and Salmaso (2010). The NPC is a method able to build multiple-feature permutation tests by means of combining joint single-feature permutation tests.

According to the ITP, when the tests on each interval of basis components (in this case: each frequency band) is performed, the adjusted p -value associated to the tests (3) on frequency h is computed as the maximum among all p -values of tests pertaining that frequency. Once the adjusted p -values are computed, we can select as significant all the frequencies with an associated adjusted p -value lower than 5%. This final selection is provided with an interval-wise control of the family wise error rate. In detail, this control means that the probability of wrongly rejecting any frequency band is lower than 5%.

Once selected the significant frequencies, the estimate of the functional moment will then be the one-year periodic function obtained by means of the Fourier expansion of the sample mean coefficients of functions φ_i , restricted to the selected frequencies. That is, if $\mathbf{v} = (v_i, \dots, v_{(Q-1)/2})$ is the index vector identifying the final selection of significant frequencies, ($v_h = 0$ if the result of the h -th test is $H_0^{(h)}$, $v_h = 1$ if the result of the h -th test is $H_1^{(h)}$), the final estimate of the functional moment is given by:

$$\hat{\mu}_\varphi(t_q) = \frac{\bar{a}^{(0)}}{2} + \sum_{h \in \mathbf{v}} \bar{a}^{(h)} \cos\left(\frac{2\pi}{Q} h t_q\right) + \bar{b}^{(h)} \sin\left(\frac{2\pi}{Q} h t_q\right), \quad (5)$$

where $\bar{a}^{(h)} = 1/n \sum_{i=1}^n a_i^{(h)}$, and $\bar{b}^{(h)} = 1/n \sum_{i=1}^n b_i^{(h)}$.

2.2 Joint propagation of aleatory and epistemic uncertainties

When both the aleatory and epistemic uncertainties are described by probability distributions, a pure probabilistic approach can be adopted for their propagation to the model output. This approach consists on the Monte Carlo sampling of possible values of all the input variables from the corresponding probability distributions and the subsequent computation of the model output in correspondence of the input values sampled Marseguerra and Zio (2002)). Random realizations of the model output can be obtained repeating a large number of times this procedure considering each time new samples of the input variables.

Instead, when the epistemic uncertainty is represented in possibilistic terms, the joint propagation of the aleatory and epistemic uncertainty can be performed by combining the Monte Carlo technique and the extension principle of fuzzy set theory by means of the following two main steps Baudrit et al. (2006): (i) repeated Monte Carlo sampling of the random variables to process aleatory uncertainty; and (ii) fuzzy interval analysis to process epistemic uncertainty.

In this work, the random variables are represented by time-varying probability distributions; therefore these two steps have to be repeated for all the time steps in the period of interest. Details of possibility theory are not reported here for brevity sake, the interested reader is referred to Dubois (2006). The operative steps of the procedure for the case study under analysis are illustrated in Appendix A.

3 Case Study

The case study that we present here concerns the design of a solar panel that provides electrical energy to a house located in the south of Spain. The size and number of the panels is a trade-off between their performance to satisfy the demand of energy and the high costs of construction and maintenance. To perform this evaluation we consider the demand of power requested by the end-users and the possibility of storing the generated exceedance power in a battery, that is necessary when the power from the solar energy is not sufficient (e.g. during cloudy days) or it is completely absent (e.g. during nights). This case study deals with a big amount of uncertainty due to the stochasticity of the behavior of the end-users, the variability of the solar irradiation, the lack of knowledge about some operation parameters of the solar panels.

The system consists of three different parts: the solar panel, the load and the battery. The power generated by the solar panel, P_S [kW], is a function of the solar irradiation, S , the number of solar cells, N , and a vector of operation parameters, $\theta = (I_{MPP}, V_{MPP}, V_{OC}, I_{SC}, N_{ot}, k_c, T_a)$ Li and Zio (2012):

$$P_S = N \cdot FF \cdot V_y \cdot I_y, \quad (6)$$

where $I_y = S \cdot I_{SC} + k_c(T_c - 25)$, $V_y = V_{OC} - k_v \cdot T_c$, $T_c = T_a + S(N_{ot} - 20)/(0.8)$, $FF = (V_{MPP} \cdot I_{MPP})/(V_{OC} \cdot I_{SC})$. I_{MPP} [A] and V_{MPP} [V] are the current

and voltage at maximum power point, respectively, V_{OC} [V] is the open circuit voltage, I_{SC} [A] is the short circuit current, N_{ot} [°C] is the nominal operating temperature, k_c [A/°C] is the current temperature coefficient, k_v [V/°C] is the voltage temperature coefficient, T_a [°C] is the ambient temperature, and the load, P_{LD} [kW], is the power demanded by the end-users.

The output model of the battery is the power, P_B [kW], that can be stored in the battery when the solar panel produces more power than the demand, i.e. when $P_{Diff} = P_S - P_{LD} > 0$, and can be given to the end-users when the opposite occurs, i.e. when $P_{Diff} = P_S - P_{LD} < 0$. In the present study we have adopted a dynamic model Chen et al. (2011) to represent the level of charge of the battery, calculating the difference between stored energies of two consecutive steps. The following equations describe the model of the battery when it is charging, i.e. $\Delta P_B(t) = -P_{Diff} < 0$ (7)-(8), when it is discharging, i.e. $\Delta P_B(t) = -P_{Diff} > 0$ (9)-(10) and when it is idle, i.e. $\Delta P_B(t) = P_{Diff} = 0$ (11).

$$-\eta_c \Delta P_B(t) \Delta t_{min} \leq K_c Q_{max}; \quad (7)$$

$$Q(t+1) = Q(t) - \eta_c \Delta P_B(t) \Delta t_{min}; \quad (8)$$

$$\Delta P_B(t) \Delta t_{min} / \eta_d \leq K_d Q_{max}; \quad (9)$$

$$Q(t+1) = Q(t) - \Delta P_B(t) \Delta t_{min} / \eta_d; \quad (10)$$

$$Q(t+1) = Q(t) - W_{hourly}. \quad (11)$$

In equations (7-11), $Q(t)$ [kWh] is the capacity of the battery at hour t , η_c and η_d are the charging and discharging efficiency, respectively, K_c and K_d are the maximum portion of rated capacity that can be added to and withdraw from storage in an hour, respectively, Q_{max} is the rated maximum stored energy, W_{hourly} [kWh] is the battery hourly discharged energy, Δt_{min} is the scheduling interval. The parameter values adopted in the model are: $\eta_c = \eta_d = 0.85$, $K_c = K_d = 0.3$, $Q_{max} = 40$, $W_{hourly} = 0.5$ kWh and $\Delta t_{min} = 1$ h. In this work, the initial level in the battery has been assumed to be equal to zero.

3.1 Uncertainty representation

In the model of the solar panel (6) the inputs can be classified in *i*) aleatory variable, i.e. the solar irradiation and the load, *ii*) epistemic variables, i.e. the operation parameters of the vector θ , and *iii*) constant, i.e. the number of solar cells N that in the present simulation has been taken equal to 30.

3.1.1 Operation parameters

The operation parameters θ are classified into parameters provided by the manufacturers, e.g. I_{MPP} , V_{MPP} , V_{OC} , I_{CS} , N_{ot} , k_c , k_v , and by the end-users, e.g. T_a . Both are associated with epistemic uncertainty, and we represent them by trapezoidal possibility distributions ($\pi^{I_{MPP}}$, $\pi^{V_{MPP}}$, $\pi^{V_{OC}}$, $\pi^{I_{CS}}$, $\pi^{N_{ot}}$, π^{k_c} , π^{k_v}) as proposed in Li and Zio (2012).

3.1.2 Solar irradiation

Solar irradiation $S[\text{kW}/\text{m}^2]$ depends on the variability of the weather. It is typically described by a probabilistic distribution, e.g. a Beta distribution, whose parameters, α and β , are inferred from sufficient historical data and are fixed for a given period Li and Zio (2012). In the present paper, coherently with the literature, we represent the solar irradiation with the Beta distribution. The main novelty of our approach with respect to the literature is that we consider the evolution of solar irradiation through time, estimating different values of the parameters α and β for each day of the year, according the method explained in Subsection 2.1.

The historical data used to elicit the parameters are daily irradiations in a geographical close area near Seville, Spain, (the square with latitude in the interval $[37, 38]$ and longitude in $[-6, -5]$), registered from July 1983 to June 2005 and stored in the database NASA: Earth Surface Meteorology for Solar Energy NASA (2008)¹. By way of example, Figure 1 shows an histogram of the historical data recorded and the correspondent Beta distribution of the solar irradiation in four different days in July and August (1st and 21st July, 11th and 31st August, respectively). The figure compares a Beta distribution characterized by constant parameters (green line), and one characterized by time-varying parameters estimated with the methodology presented in Subsection 2.1 (red line). We observe from the histograms that the distribution of solar irradiation is changing through time even in the relatively small period of two months. Hence, a correct approach to model such irradiation data is to consider its time-varying distribution, rather than a constant one.

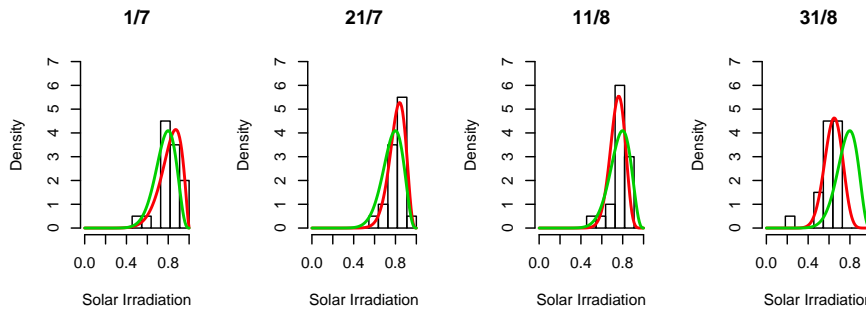


Figure 1: Histogram of the recorded data and the correspondent Beta distribution for the 1st and 21st of July, 11th and 31st of August, and corresponding Beta distributions characterized by: constant parameters (green line); time-varying parameters (red line).

We suppose that, for a fixed day t_q , the observed data $S_i(t_q)$ is a random

¹These data were obtained from the NASA Langley Research Center Atmospheric Science Data Center Surface meteorological and Solar Energy (SSE) web portal supported by the NASA LaRC POWER Project. Data are freely available at: NASA Surface Meteorology and Solar Energy, A Renewable Energy Resource web site (release 6.0): <http://eosweb.larc.nasa.gov>

independent sample from a beta distribution of parameters $\alpha(t_q)$ and $\beta(t_q)$:

$$S_i(t_q) \sim \text{Beta}(\alpha(t_q), \beta(t_q)), \quad \forall i = 1, \dots, 22, q = 1, \dots, 365. \quad (12)$$

To estimate the time-varying parameters we adopt the methodology discussed in Subsection 2.1. Since we need to estimate, for each t_q , the two parameters $\alpha(t_q)$ and $\beta(t_q)$, we need to estimate the mean and variance of the data distribution, for each time unit t_q .

3.1.3 Load

The load, P_{LD} , is affected by aleatory uncertainty since its value depends on the behavior of the end-users. Typically it is modeled by a normal probabilistic distribution Liu et al. (2011), with parameters inferred from the large amount of historical data available. In this work, we use a normal distribution, estimating two different time-varying mean values for days and nights, μ_{day} , and μ_{night} , respectively, following the procedure explained in Subsection 2.1, and maintaining a same standard deviation σ .

As well as the solar irradiation, also the load P_{LD} [kW] has a time varying structure. In particular, we suppose that, for each day of the year t_q , the load has two normal distributions for days and nights, with the same constant standard deviation ($\sigma = 0.25$ kW) and two time-varying means ($\mu_{P_{LD},day}(t_q)$ and $\mu_{P_{LD},night}(t_q)$, respectively). The model assumed for the daily and nightly load, for each time t_q is then the following:

$$P_{LD,day/night}(t_q) \sim N(\mu_{P_{LD,day/night}}(t_q), \sigma^2), \quad q = 1, \dots, Q. \quad (13)$$

To estimate the daily and nightly mean functions, it is not possible to proceed applying the ITP to the daily load data, as they are not directly available. The daily mean electrical consumption of a house in the south of Spain is about 24.54 kWh Sech-Spahousec (2011) and in the night the demand of electricity is the half than during the day Omie (2012). Thus, the estimated means of the hourly load for days and nights are 1.363 kW and 0.682 kW, respectively. Since these data are aggregated through the entire year, it is not possible to infer a time varying distribution. Consequently, a different approach is here necessary.

Most of the usual household electrical devices (e.g. washing machine, refrigerator, TV) are approximately used in the same way in summer and winter, and, thus, their electrical consumption can be assumed to follow a constant distribution throughout the year. The only devices that may have a time-varying load are the air conditioning systems (whose load varies in the warm months depending on the external temperature) and the lighting (whose load changes through the year depending on the variation of daylight time). Since for the former, the load is higher than for the latter, we consider only the air conditioning systems (AC) as a device with a time varying load. Since the AC load depends on the external temperature, we first apply the ITP to minimum and maximum daily

temperatures, to find a smooth time-varying estimate of their mean functions. Then, we use this estimate to calculate the time-varying daily and nightly means of the load due to the AC. The steps of the procedure applied to calculate the load are detailed in Appendix B.

3.2 Uncertainty propagation

The joint propagation of aleatory and epistemic uncertainties represented by probability and possibility distributions, respectively, is carried out by Monte Carlo simulation and Fuzzy Interval Analysis. Since the analysis is time-varying, the procedure is repeated for each time steps in the period of interest.

In the present case study, the aleatory variables are the solar irradiation and the loads that vary during days and nights. As a consequence of their variation, the level of energy in the storage system varies too. We assume that at the first time step it is day (i.e., there is solar irradiation) and the level of energy in the storage system is equal to zero.

When the power generated by the solar panel is higher than the demands of the end-users, the level of energy in the storage system increases and the end-users are satisfied (the energy not supplied (ENS) is equal to zero); instead when the power generated is lower than the demands of the end-users two cases can occur: 1) there is enough energy in the storage system to supply the end-users, so the level in the storage decreases but the end-users are satisfied (the ENS is equal to zero); 2) there is not enough energy in the storage system, so the level in the storage decreases to zero (if it is not already zero) and the ENS to the end-users is positive.

The following time steps have been considered in our case:

- $\Delta t_{min} = 1[\text{h}]$ is the smallest time step of the system model. The total number of hours in the period of interest is defined by the variable N_{steps} ;
- $\Delta t_{max} = 12[\text{h}]$ is the time interval in which the power generated by the solar panel, P_S , and the one demanded by the end-users, P_{LD} , can be considered constant. This assumption has been introduced to reduce the computational time of the simulation and to distinguish only between day and night, and is coherent with the calculation of P_{LD} proposed in Subsection 3.1.3. Therefore, the total number of different values considered for those variables is $N_{steps}/\Delta t_{max}$.

The joint uncertainty propagation that consists in combining Monte Carlo technique with the extension principle of fuzzy set theory is illustrated in details in Appendix A with respect to the case study considered in this work. At the end of the procedure an ensemble of m fuzzy random realizations (fuzzy intervals) π_{EENS}^k , $k = 1, \dots, m$, of the Expected Energy Not Supplied (EENS) index is obtained.

On the basis of the rule of the possibility theory Baudrit et al. (2006), these possibilistic distributions can be aggregated. As a result, two cumulative distribution functions (cdfs), called belief and plausibility (i.e., the lower and upper cdfs, respectively), of the Expected Energy Not Supplied are obtained. They can be interpreted as bounding cumulative distribution functions Baudrit et al. (2006) and they contain all the possible cumulative distribution functions that can be generated by a pure probabilistic approach that considers all the inputs variables as probabilistic. For the sake of comparison, we have embraced also this method with $m = 10000$ samples of the probabilistic variables: in this case, the possibilistic distributions of the input variables are transformed into probabilistic distributions by the normalization method given in Flage et al. (2008).

3.3 Results

The adjusted p -values for the first and second moments are reported in the top panels of Figure 2, where the 5% level is indicated as a horizontal red line. For the first moment, the p -values associated to the first three frequencies are lower than the chosen significance level (and are, furthermore, lower than every typically-used significance level), whereas all other p -values are higher. Hence, we have a rejection corresponding to the mean value (zero-frequency) and the sine and cosine functions of period one year. For the second moment we have instead a rejection on the first four frequencies, corresponding to the mean value and the sine and cosine functions of period one year, six and three months. The final estimates are periodic functions fully described by the sample means coefficients on these frequencies.

To appreciate the result of the test, the lower panels of Figure 2 show, for the first two moments, the two estimates of the mean: ITP estimate (red) and daily estimate (black). Gray lines are the solar irradiation data in southern Spain for the first moment (left), and squared solar irradiances for the second moment (right). Comparing the ITP and daily estimates, it can be seen that the first method gives smooth curves, which follow the yearly fluctuations of the quantity of interest, whereas the second one gives extremely irregular functions.

The results of the analysis on the min-max temperature data, and the subsequent results of the load parameters are presented in Figure 3. On the top, the ITP-adjusted p -values for the minimum (left) and maximum (right) temperatures are reported. In this case, the ITP selects as significant the mean value and the first two frequencies, both for the min and the max temperatures. On the middle, the daily minimum and maximum temperatures data in southern Spain (light blue and red lines, respectively) are shown, together with the ITP estimates of the two functional means, evaluated according to the ITP results. The horizontal line indicates the threshold temperature at which the AC is turned on, $T_{thres} = 26^\circ\text{C}$. On the bottom panel, the estimates of the time-varying means of the load, for days and nights (yellow and black lines, respectively) are reported. To appreciate how the modeling of the load data is related to the test results,

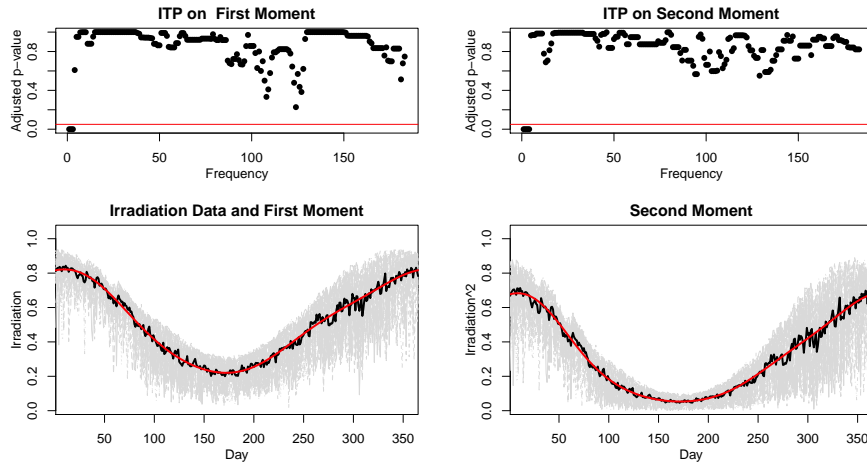


Figure 2: Top: ITP-adjusted p -values for each frequency of the Fourier expansion for the first (left) and second (right) moment. Bottom: ITP (red) and daily (black) estimates of the first two moments. Gray lines: solar irradiation (left); and squared solar irradiation (right).

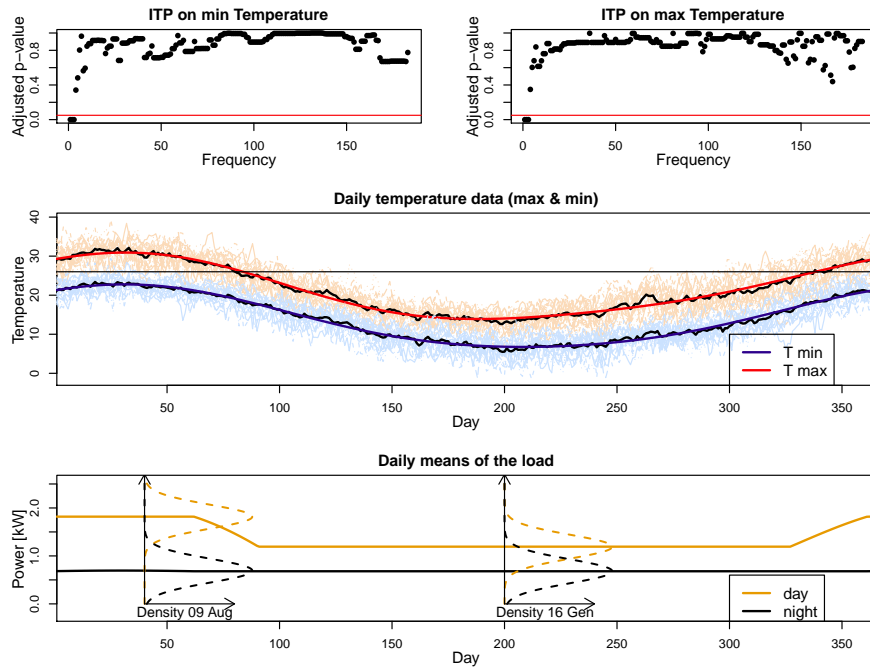


Figure 3: Top: ITP-adjusted p -values for each frequency of the Fourier expansion for the min (left) and max (right) temperatures. Middle: daily min (light blue) and max (light red) temperatures data and ITP estimates for the means (bold blue and red lines). Bottom: estimates of the time-varying means of the load for days (yellow) and nights (black), and densities of simulated data in a summer and winter day.

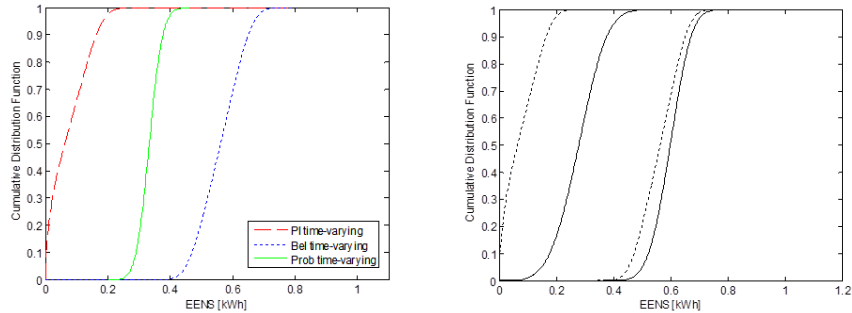


Figure 4: Left: comparison of the cumulative distribution functions of the EENS [kWh] obtained by the pure probabilistic approach (solid line) with the belief (dotted line) and plausibility (dashed line) functions obtained by the Monte Carlo and Fuzzy Interval Analysis. Right: comparison of the lower and upper cumulative distribution functions of the EENS obtained by the Monte Carlo and Fuzzy Interval Analysis approach considering constant (solid line) and time-varying (dotted line) parameters of the probabilistic distribution.

the figure indicates the densities of the simulated day and night load $P_{LD,day}(t_q)$ and $P_{LD,night}(t_q)$ for a summer and a winter day. Note that the variability of the normal distribution remains constant, whereas its mean level changes from days and nights, and from winter to summer.

Monte Carlo simulation and Fuzzy Interval Analysis approach (Subsection 3.2 and Appendix A) considering the time-varying parameters of the probabilistic distribution of the solar irradiation and of the loads determined above. The analysis has been carried out with respect to the month of July that is a critical period for the high demand of power by the end-users. In fact, the hot temperature reached in the south of Spain gives rise to a large use of air conditioners. Figure 4 reports on the left panel a comparison of the cumulative distribution functions of the EENS index obtained by the probabilistic uncertainty propagation approach (solid lines) with the belief (lower curves) and plausibility (upper curves) functions (see Subsection 3.2).

The Monte Carlo and Fuzzy Interval Analysis method explicitly propagates the aleatory and epistemic uncertainty: the separation between the belief and plausibility functions reflects the imprecision in the knowledge of the possibilistic variables and the slope pictures the variability of the probabilistic variables. Instead, the uncertainty in the output distribution of the pure probabilistic approach is given only by the slope of the cumulative distribution. As expected, the cumulative distribution of the EENS obtained by the pure probabilistic method is within the belief and plausibility functions obtained by the Monte Carlo and Fuzzy Interval Analysis approach.

Figure 4 (on the right) compares the previous results, carried out with the Monte Carlo and Fuzzy Interval Analysis approach, with those obtained by the same method but by considering constant the parameters of the probabilistic distributions of the solar irradiation S , and the loads P_{LD} . A conservative

measure of the EENS distribution to be used to evaluate the size of the panel can be chosen as the 99th percentile of the distribution. The lower and upper values of this measure, obtained with time-varying or constant parameters, are reported in Table 1. The value obtained by considering time-varying parameters (with a model that describes with a higher precision the real climatic conditions) are lower than the ones obtained with constant parameters.

	EENS	
	Lower value [kWh]	Upper value [kWh]
Time-varying	0.22	0.70
Constant	0.45	0.78

Table 1: Lower and upper values of the 99th percentile of the EENS distribution, evaluated with time-varying and constant parameters.

It can be seen that the lower and upper cumulative distributions functions obtained by considering time-varying parameters are always lower than those resulted by keeping constant those parameters. This means that in this case study a time-varying analysis allows designing the solar panel with smaller dimension. Furthermore, the gap between the cumulative distributions functions obtained by considering time-varying parameters is higher than that between the curves obtained by keeping constant those parameters. In particular, by considering time-varying parameters, we introduce a higher variability on the EENS estimation, due to the fact that the distribution of data changes daily. The higher variability allows considering within our model the situation in which the solar panel fully support the load demand, including the zero value in the EENS distribution.

4 Conclusions

We illustrated a methodology to represent and propagate the aleatory and epistemic uncertainties of renewable energy generation systems. We represented the former ones by probability distributions and the second ones by possibility distributions. In particular, we focused on the aleatory variables that present a time-varying behavior (e.g., solar irradiation and loads) and we elicited time-varying probability distributions from historical climatic data.

Once all uncertainties have been represented, we proceeded to evaluate the output of interest (e.g., the Expected Energy Not Supplied) by propagating the uncertainties through the model of the energy distribution system. The results that can be obtained from this analysis can provide a support in the decision process for the dimensioning of the energy generation system.

In this work, we applied the methodology to a model of an energy system made of a solar panel, a storage energy system and the loads. In particular, we considered the variations in time of the solar irradiation and the loads, describing

them by probabilistic distributions with time-varying parameters. We evaluated the Expected Energy Not Supplied as a quantitative indicator of the analysis.

Two main results have to be highlighted. The first one concerns the uncertainty propagation method that divides the contribution of the aleatory and epistemic uncertainty, identifying upper and lower bounds of the EENS, i.e., an interval of values of the EENS for a given confidence level. This can be of interest in the decision making process to identify the proper size of the solar panel. The second result shows that accounting for time-varying parameters in the distributions of the solar irradiation and of the loads leads to more realistic results that, in this case, allows to reduce the dimension of the solar panel. Thus, considering constant parameters an overestimation of the size of the solar panel can be done.

References

- Atwa, Y. M., El-Saadany, E. F., Salama, M. M. A. and Seethapathy, R. (2010), Optimal renewable resources mix for distribution system energy loss minimization, *Power Systems, IEEE Transactions on* **25**(1), 360–370.
- Aven, T. and Zio, E. (2011), Some considerations on the treatment of uncertainties in risk assessment for practical decision making, *Reliability Engineering & System Safety* **96**(1), 64–74.
- Baraldi, P. and Zio, E. (2008), A combined monte carlo and possibilistic approach to uncertainty propagation in event tree analysis, *Risk Analysis* **28**(5), 1309–1326.
- Baudrit, C., Dubois, D. and Guyonnet, D. (2006), Joint propagation and exploitation of probabilistic and possibilistic information in risk assessment, *Fuzzy Systems, IEEE Transactions on* **14**(5), 593–608.
- Billinton, R., Allan, R. N. and Allan, R. N. (1984), *Reliability evaluation of power systems*, Vol. 2, Plenum press New York.
- Borges, C. L. (2012), An overview of reliability models and methods for distribution systems with renewable energy distributed generation, *Renewable and sustainable energy reviews* **16**(6), 4008–4015.
- Chen, C., Duan, S., Cai, T., Liu, B. and Hu, G. (2011), Optimal allocation and economic analysis of energy storage system in microgrids, *Power Electronics, IEEE Transactions on* **26**(10), 2762–2773.
- Dubois, D. (2006), Possibility theory and statistical reasoning, *Computational statistics & data analysis* **51**(1), 47–69.
- ENEA (2006), ‘I condizionatori dell’aria: raffrescatori e pompe di calore’, Ente per le Nuove Tecnologie, l’Energia e l’Ambiente.

- Ferraty, F. and Vieu, P. (2006), *Nonparametric functional data analysis: theory and practice*, Springer.
- Flage, R., Aven, T. and Zio, E. (2008), Alternative representations of uncertainty in system reliability and risk analysis-review and discussion, in ‘European Safety and Reliability Conference (ESREL), Valencia, SPAIN’, Vol. 43, pp. 22–25.
- FreeMeteo (2012), ‘Hourly weather history for barcelona, spain. station reporting: Sevilla/san pablo’, <http://freemeteo.com>.
- Helton, J. C. and Oberkampf, W. L. (2004), Alternative representations of epistemic uncertainty, *Reliability Engineering & System Safety* **85**(1), 1–10.
- INE (2008), ‘Instituto nacional de estadísticas: Encuesta de hogares y medio ambiente 2008’, <http://www.ine.es/jaxi>.
- Izquierdo, M., Moreno-Rodríguez, A., González-Gil, A. and García-Hernando, N. (2011), Air conditioning in the region of madrid, spain: An approach to electricity consumption, economics and co2 emissions, *Energy* **36**(3), 1630–1639.
- Klir, G. J. and Yuan, B. (1995), *Fuzzy sets and fuzzy logic, theory and applications*, Upper Saddle River, NJ: Prentice-Hall.
- Li, Y. and Zio, E. (2012), Uncertainty analysis of the adequacy assessment model of a distributed generation system, *Renewable Energy* **41**, 235–244.
- Liu, Z., Wen, F. and Ledwich, G. (2011), Optimal siting and sizing of distributed generators in distribution systems considering uncertainties, *Power Delivery, IEEE Transactions on* **26**(4), 2541–2551.
- Marseguerra, M. and Zio, E. (2002), *Basics of the Monte Carlo method with application to system reliability*, LiLoLe - Verlag GmbH, Hagen, Germany.
- NASA (2008), ‘Surface meteorology and solar energy, a renewable energy resource web site (release 6.0)’, <http://eosweb.larc.nasa.gov/sse>.
- Omie (2012), ‘Precio orario del mercado diario’, <http://www.omie.es>.
- Pesarin, F. and Salmaso, L. (2010), *Permutation tests for complex data: theory, applications and software*, John Wiley & Sons Inc.
- Pini, A. and Vantini, S. (2013), The interval testing procedure: Inference for functional data controlling the family wise error rate on intervals., Technical Report 13/2013, MOX, Politecnico di Milano.
- Ramsay, J. O. and Silverman, B. W. (2002), *Applied functional data analysis: methods and case studies*, Vol. 77, Springer.

Ramsay, J. O. and Silverman, B. W. (2005), *Functional data analysis*, Springer, New York.

Salameh, Z. M., Borowy, B. S. and Amin, A. R. A. (1995), Photovoltaic module-site matching based on the capacity factors, *IEEE Trans. on Energy Conversion* **10**(2), 326–332.

Sech-Spahousec (2011), ‘Análisis del consumo energético del sector residencial en españa’.

A Joint uncertainty propagation

The operative steps of the procedure for the joint uncertainty propagation by Monte Carlo simulation and Fuzzy Interval Analysis are here detailed with respect to the case study presented in Section 3. As a quantitative indicator of the analysis, the Expected Energy Not Supplied index is computed.

1. Set $k = 1$ (outer loop processing aleatory uncertainty).
2. Sample the solar irradiations \tilde{S}_l^k , $l = 1, \dots, N_{steps}/\Delta t_{max}$ from Beta distribution (equation (1)) if l is an odd number (i.e. when it is day), otherwise, set $\tilde{S}_l^k = 0$ (i.e. when it is night). Then, sample the loads $\tilde{P}_{LD,l}^k$, $l = 1, \dots, N_{steps}/\Delta t_{max}$ from equation (13) taking into account the different distributions associated with that variable during the days and nights. The vectors $[\tilde{\mathbf{S}}^k]_l$ and $[\tilde{\mathbf{P}}_{LD}^k]_l$, are transformed into $[\tilde{\mathbf{S}}^k]_j$ and $[\tilde{\mathbf{P}}_{LD}^k]_j$, $j = 1, \dots, N_{steps}$, respectively, repeating each value Δt_{max} times, to obtain values of solar irradiations and loads for each hour in all the period of interest.
3. Set $\alpha = 0$ (middle loop processing epistemic uncertainty).
4. Set $j = 1$ (inner loop processing the time variation).
5. Select the corresponding α -cuts of the possibility distributions ($\pi^{I_{MPP}}$, $\pi^{V_{MPP}}$, $\pi^{V_{OC}}$, $\pi^{I_{CS}}$, $\pi^{N_{ot}}$, π^{k_c} , π^{k_v}) as intervals of possible values of the possibilistic variables I_{MPP} , V_{MPP} , V_{OC} , I_{CS} , N_{ot} , k_c , k_v .
6. Calculate the smallest and largest values of the solar power generated, $\underline{P}_{S,j,\alpha}^k$ and $\overline{P}_{S,j,\alpha}^k$, respectively, by equation (6) considering the fixed values S_j^k sampled for the random variables S and all values of the possibilistic variables I_{MPP} , V_{MPP} , V_{OC} , I_{CS} , N_{ot} , k_c , k_v in the α -cuts of their possibility distributions.
7. Compute the value $\underline{P}_{Diff,j,\alpha}^k = \underline{P}_{S,j,\alpha}^k - P_{j,k}^L$: if $\underline{P}_{Diff,j,\alpha}^k > 0$, go to step 7.a.; if $\underline{P}_{Diff,j,\alpha}^k < 0$ go to step 7.b., else go to step 7.c.:

- a. set to zero the Energy Not Supplied index, $\overline{ENS}_{j,\alpha}^k = 0$, and increase the level of energy in the battery by equation (8), $\underline{Q}_{j+1,\alpha}^k = f(Q_{j,\alpha}^k, \underline{P}_{B,j,\alpha}^k, \eta_c)$, where $\underline{P}_{B,j,\alpha}^k = -\underline{P}_{Diff,j,\alpha}^k$ if the constraint defined in equation (7) is verified, otherwise it is computed by equation (7). If the level of energy in the battery at the step $j+1$ is higher than its maximum capacity, i.e. $\underline{Q}_{j+1,\alpha}^k > Q_{max}$, then, set $\underline{Q}_{j+1,\alpha}^k = Q_{max}$;
 - b. decrease the level of energy in the battery by equation (10), $\underline{Q}_{j+1,\alpha}^k = f(Q_{j,\alpha}^k, \underline{P}_{B,j,\alpha}^k, \eta_d)$; if the constraint defined in equation (9) is verified $\underline{P}_{B,j,\alpha}^k = -\underline{P}_{Diff,j,\alpha}^k$ (case i.), otherwise $\underline{P}_{B,j,\alpha}^k$ is computed by equation (9) (case ii.). If the level of energy in the battery at the step $j+1$ is higher than zero, the Energy Not Supplied index is computed as $\overline{ENS}_{j,\alpha}^k = 0$ for the case i., and $\overline{ENS}_{j,\alpha}^k = -\underline{P}_{Diff,j,\alpha}^k - \underline{P}_{B,j,\alpha}^k$ for the case ii.; otherwise, set, $\underline{Q}_{j+1,\alpha}^k = 0$ and $\overline{ENS}_{j,\alpha}^k = -\underline{P}_{Diff,j,\alpha}^k$;
 - c. set $\overline{ENS}_{j,\alpha}^k = 0$, and decrease the level of the battery by equation (11), $\underline{Q}_{j+1,\alpha}^k = f(Q_{j,\alpha}^k, W_{hourly})$. If the level of energy in the battery at the step $j+1$ is lower than zero, then set $\underline{Q}_{j+1,\alpha}^k = 0$.
8. Repeat step 7. for the evaluation of the lower bounds of $\underline{ENS}_{j,\alpha}^k$, computing the upper values of $\overline{P}_{Diff,j,\alpha}^k$, $\overline{P}_{B,j,\alpha}^k$ and $\overline{Q}_{j,\alpha}^k$.
 9. If $j \leq N_{steps}$, then set $j = j+1$ and return to step 5.; otherwise go to step 10.
 10. Compute the total lower and upper bounds of the ENS index in the period under analysis as $\underline{ENS}_{\alpha}^k = \sum_{j=1}^{N_{steps}} \underline{ENS}_{j,\alpha}^k$, $\overline{ENS}_{\alpha}^k = \sum_{j=1}^{N_{steps}} \overline{ENS}_{j,\alpha}^k$; the lower and upper bounds of EENS, $\underline{EENS}_{\alpha}^k$ and $\overline{EENS}_{\alpha}^k$, are obtained by performing the means of $\underline{ENS}_{\alpha}^k$ and $\overline{ENS}_{\alpha}^k$, respectively.
 11. Take the extreme values, $\underline{EENS}_{\alpha}^k$ and $\overline{EENS}_{\alpha}^k$, found in 10. as the lower and upper limit of the α -cut of the Expected Energy Not Supplied.
 12. If $\alpha \neq 1$, then set $\alpha = \alpha + \Delta\alpha$ and return to step 4. to compute the EENS for another α -cut; otherwise a fuzzy random realization, π_{EENS}^k , of the EENS has been identified. If $k \neq m$, where m is the number of simulations, then set $k = k+1$ and return to step 2.; else stop the algorithm.

At the end of the procedure the fuzzy random realizations (fuzzy intervals) π_{EENS}^k , $k = 1, \dots, m$ of the Expected Energy Not Supplied index is constructed as the collection of the values $\underline{EENS}_{\alpha}^k$ and $\overline{EENS}_{\alpha}^k$, found at step 10. (in other words, π_{EENS}^k is defined by all its α -cut intervals $(\underline{EENS}_{\alpha}^k, \overline{EENS}_{\alpha}^k)$).

B Time-varying estimate of the load

The operative steps of the procedure applied to find time-varying estimates of the load is briefly described here. Starting from the daily minimum and maximum temperatures in the Seville area, stored in the NASA data base NASA (2008), we calculate the time-varying mean of the load of an AC with some fixed characteristics. We consider a class “A” device, with an Energy Efficiency Ratio (EER) equal to 3.5. The number of AC installed in the house is set equal to the mean number of conditioners in Spanish homes in Andalusia, which is 1.623 INE (2008). The nominal power of the AC is calculated as $P_N^{AC} = Surf \cdot Ceiling \cdot 25$ ENEA (2006), where $Surf = 20m^2$ is the surface of the room and $Ceiling = 2.7m$ is the height of the ceiling. All data are chosen to indicate a representative Spanish house. Finally, since the proportion of Spanish that leave the AC turned on at night is equal to 7.6% INE (2008), we multiply the AC load at nights by this proportion.

In order to calculate the mean load of such AC system, first of all, we find functional estimates for the mean tendency of the daily minimum and maximum temperature for the given location ($T_{min}(t_q)$ and $T_{max}(t_q)$ [$^{\circ}C$], respectively), by means of the ITP on min and max temperatures, with the methodology presented in Subsection 2.1. Then, for each day t_q , we perform the following calculation:

- We fix a threshold temperature $T_{thres} = 26^{\circ}C$, and suppose that the AC is turned on when the external temperatures exceed the threshold, as in Izquierdo et al. (2011).
- We estimate the daily lapse of time in which the AC is turned on $h_{on}(t_q)[h]$, supposing for each day a linear temperature profile between $T_{min}(t_q)$ and $T_{max}(t_q)$:

$$h_{on}(t_q) = 24 \left(\frac{T_{max}(t_q) - T_{thres}}{T_{max}(t_q) - T_{min}(t_q)} \right). \quad (14)$$

This approximation is justified by the comparison of our results with a daily temperature profile estimated from hourly data FreeMeteo (2012).

- The quantity $h_{on}(t_q)$ is then divided into daily (10.00 a.m. - 10.00 p.m.) and nightly (10.00 p.m. - 10.00 a.m.) hours of switching on ($h_{on}^{day}(t_q)$ and $h_{on}^{night}(t_q)$, respectively), assuming that $T_{max}(t_q)$ is attained at 4.00 p.m. and $T_{min}(t_q)$ at 6.00 a.m. FreeMeteo (2012).
- The mean power load on days of the AC is then calculated as:

$$\mu_{P_{LD,day}}(t_q) = P_N^{AC} n_{room} h_{on}^{day}(t_q) / (12EER) \quad (15)$$

The mean load on nights, is:

$$\mu_{P_{LD,night}}(t_q) = P_N^{AC} n_{room} h_{on}^{night} \cdot 0.076(t_q) / (12EER) \quad (16)$$

Note that both quantities are divided by 12[h] in order to found an estimate of the hourly power.

- The quantities $\mu_{P_{LD},day}$ and $\mu_{P_{LD},night}$ are finally added to the day and night fixed averages (mean load without AC), calculated in order to maintain the values of 1.363 kW and 0.682 kW as yearly means.

MOX Technical Reports, last issues

Dipartimento di Matematica “F. Brioschi”,
Politecnico di Milano, Via Bonardi 9 - 20133 Milano (Italy)

- 54/2014 FERRARIO, E.; PINI, A.
Uncertainties in renewable energy generation systems: functional data analysis, monte carlo simulation, and fuzzy interval analysis
- 53/2014 IEVA, F.; PAGANONI, A.M., PIETRABISSA, T.
Dynamic clustering of hazard functions: an application to disease progression in chronic heart failure
- 52/2014 DEDE , L.; QUARTERONI, A.; S. ZHU, S.
Isogeometric analysis and proper orthogonal decomposition for parabolic problems
- 51/2014 DASSI, F.; PEROTTO, S.; FORMAGGIA, L.
A priori anisotropic mesh adaptation on implicitly defined surfaces
- 50/2014 BARTEZZAGHI, A.; CREMONESI, M.; PAROLINI, N.; PEREGO, U.
An explicit dynamics GPU structural solver for thin shell finite elements
- 49/2014 D. BONOMI, C. VERGARA, E. FAGGIANO, M. STEVANELLA, C. CONTI, A. REDAELLI, G. PUPPINI ET AL
Influence of the aortic valve leaflets on the fluid-dynamics in aorta in presence of a normally functioning bicuspid valve
- 48/2014 PENTA, R; AMBROSI, D; SHIPLEY, R.
Effective governing equations for poroelastic growing media
- 47/2014 PENTA, R; AMBROSI, D; QUARTERONI, A.
Multiscale homogenization for fluid and drug transport in vascularized malignant tissues
- 46/2014 PENTA, R; AMBROSI, D.
The role of the microvascular tortuosity in tumor transport phenomena
- 45/2014 PEZZUTO, S.; AMBROSI, D.; QUARTERONI, A.
An orthotropic active-strain model for the myocardium mechanics and its numerical approximation